Numerical Analysis of a Paraffin/Metal Foam Composite for Thermal Storage

Numerical Analysis of a Paraffin/Metal Foam Composite for Thermal Storage

P Di Giorgio*, M Iasiello, A Viglione*, M Mameli*[,1], S Filippeschi*, P Di Marco*, A Andreozzi**, N Bianco****

*DESTEC – University of Pisa – Largo L. Lazzarino 2-56122 – Pisa
**DII, University of Naples - Federico II, P.le Tecchio, 80, 80125 - Naples

[1] E-mail: mauro.mameli@ing.unipi.it

Abstract. In the last decade, the use of Phase Change Materials (PCMs) as passive thermal energy storage has been widely studied both analytically and experimentally. Among the PCMs, paraffins show many advantages, such as having a high latent heat, a low vapour pressure, being chemically inert, stable and non-toxic. But, their thermal conductivity is very low with a high volume change during the melting process. An efficient way to increase their poor thermal conductivity is to couple them with open cells metallic foams. This paper deals with a theoretical analysis of paraffin melting process inside an aluminum foam. A mathematical model is developed by using the volume-averaged governing equations for the porous domain, made up by the PCM embedded into the metal foam. Non-Darcian and buoyancy effects are considered in the momentum equation, while the energy equations are modelled with the Local Thermal Non-Equilibrium (LTNE) approach. The PCM liquefaction is treated with the apparent heat capacity method and the governing equations are solved with a finite-element scheme by COMSOL Multiphysics®. A new method to calculate the coupling coefficients needed for the thermal model has been developed and the results obtained have been validated comparing them to experimental data in literature.

1.Introduction

In the last years, the wide diffusion of technologies that can produce thermal energy from renewable and intermittent sources has increased the need for an efficient TES. Phase-change-materials (PCMs), which release or absorb thermal energy during melting and solidification process, are particularly attractive in this field, since they allow to exchange heat virtually at constant temperature and because of their high thermal energy storage density. However, most PCMs presents the common problem of low thermal conductivity, (around $\mathbf{0.2\ W/mK}$ for most paraffin waxes) that strongly limits the energy charging/discharging rates. Therefore, the introduction of highly conductive materials embedded with PCMs has been already proposed in literature in order to improve the heat exchange process [1]. Metal foams with their low relative density and relatively high thermal conductivity are believed to be a promising material for enhancing heat transfer performance and reducing the charging and discharging periods of PCMs. A significant amount of studies on the thermal conductivity enhancement of PCMs focused on use of porous matrices. Tian and Zhao [2] numerically and experimentally investigated the heat transfer behaviour with a paraffin wax embedded in a copper metallic foam, showing that the addition of the foam can increase the overall heat transfer rate by three to ten times (depending on the metal foam structures and materials) during the melting process. Tong et al [3] inserted an open cell aluminum foam matrix into liquid water and investigated the heat transfer rate during the icing process. Results show that the thermal power exchanged with water during the solidification process is three

times higher with the foam. Mancin et al. [4] tested three paraffin waxes with different melting points temperatures (53, 57, 59°C) embedded into a copper metal foam. The experimental results clearly show that the heat transfer capability was improved by a factor of 4 to 8 depending on the metal foam characteristics. Moreover, several mathematical models of the phase change process of a PCM embedded in metallic foam can be found in literature: Alshaer et al. [5] presented a model of the heat exchange in a carbon foam matrix saturated with a PCM. The model was obtained by the Volume Averaging Technique (VAT) based on single-domain energy equation. Mathematical model was validated by comparing its prediction with previous experimental measurements and good agreement was obtained.

Interesting studies with the aim to characterize the foam properties influence on the PCM melting process were carried out by Osama Mesalhy et al. [6] and Lafdi et al [7].In the first one the authors developed a numerical model solving the convection motion of the liquid phase inside a porous matrix, considering Darcy, Brinkman and Forcheimer effects and applying a two energy equations model. The coupling coefficient was estimated simplifying the heat transfer between the foam and the PCM with the heat conduction between two cylindrical layers. In the second paper, the authors experimentally investigated the thermal behaviour of the PCM melting process inside various aluminium foams, finding out that with high porosity and low PPI foams the steady-state regime is reached faster due to the natural convection effect.

The present study aims at developing a robust mathematical model based on the Volumes Of Fluid (VOF) method and the Volume Averaging Technique (VAT) using the non-thermal equilibrium approach, with physically based coefficients and a reasonable computational cost, in order to analyse and predict the phase change process characteristics with different metal foam properties. In particular, a novel approach for the esteem of the interfacial heat transfer coefficient between the solid matrix and the PCM is proposed. The model is qualitatively validated against experimental data in the literature and finally, a simulation in microgravity condition is performed in order to understand what the effect of convection on the overall heat transfer rate is.

2. Model description

2.1. Metal foam models

In order to characterize the heat exchange between metal foam and PCM a 3D model of the foam is necessary. The best foam model in literature was developed by Weaire and Phelan in 1994 [8]. They proposed a new foam element structure, based on eight polyhedrae of equal volume, but different face number. The other foam model widely used in literature is the Kelvin one (see figure 1), that in 1887 proposed a polyhedron with 14 slightly curved faces (eight hexagons and six squares). Because of the easier implementation of Kelvin model, several studies focused on the comparison between the two models: Cunsolo et al. [9] demonstrated that for an air flow there is no significant differences between the two models in case of high porosity foam. For this reason, Kelvin model described and characterized by Iasiello et al. [10] has been chosen. Their work was based on a comparison between simulations made on real foam geometries (obtained with topographical analysis) and ideal Kelvin's ones designed with Surface Evolver. The final obtained open-cell foam element is represented in figure 1.

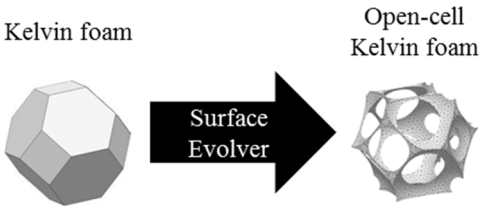

Figure 1. Kelvin model used for metal foam representation modeled with Surface Evolver.

2.2. Modeling approach and basic equations

The model is implemented by using the Volume Averaging Technique (VAT). The variables resolved in the balance equations are averaged on a Representative Volume Element (REV), which can be

generally defined as the smallest volume of a porous material for which the continuum assumption is valid [11].

The metal foam-paraffin system is reduced to an equivalent, homogeneous and isotropic porous medium. Two temperature fields are resolved by using a Local Thermal Non-Equilibrium (LTNE) model: one for the metal foam and one for the paraffin.

The numerical model presents the following assumptions:

- The PCM is modeled using the apparent heat capacity method. The temperature dependence of specific heat is described as a continuous function (such as a continuous Dirac Delta function), whose integral is equal to the latent heat. The temperature at which the melting process begins is $T_{start-melt}$, while it ends at $T_{end-melt}$.
- Paraffin viscosity and buoyancy forces are defined trough a step function.
- The liquid PCM is considered incompressible and Newtonian, and subjected to the Boussinesq's approximation.
- The natural convection starts in a REV only when the paraffin is completely melted.
- The changes of density of the paraffin during the whole melting process are neglected. This approximation can be made since the highest impregnation ratio achievable is given by the liquid and solid density ratio. For this reason, only the liquid density is considered. Impregnation ratio is defined as the ratio between the mass of PCM embedded in the metal foam and the theoretic mass.

$$IR = m_{PCM}/(\rho_{PCM}\varepsilon V) \tag{1}$$

The volume averaged equations [11] are:

$$\frac{\partial\langle\rho_{PCM}\rangle}{\partial t} + \nabla\cdot\langle\rho\bar{v}\rangle_{PCM} = 0 \tag{2}$$

$$\frac{\rho}{\varepsilon}\left(\frac{\partial\langle\bar{v}\rangle}{\partial t} + \frac{1}{\varepsilon}\nabla\cdot(\langle\bar{v}\rangle\langle\bar{v}\rangle)\right) = -\nabla\langle p\rangle + \frac{\mu}{\varepsilon}\nabla\cdot(\nabla\langle\bar{v}\rangle) + \rho\beta\bar{g}(\langle T\rangle_{PCM} - T_{start-melt}) - \frac{\mu}{\bar{\bar{K}}}\langle\bar{v}\rangle - \frac{\rho C_F}{\sqrt{\bar{\bar{K}}}}|\langle\bar{v}\rangle|\langle\bar{v}\rangle \tag{3}$$

$$\varepsilon\left(\rho C_p\right)_{PCM}\left(\frac{\partial\langle T\rangle_{PCM}}{\partial t} + \bar{v}\cdot\nabla\langle T\rangle_{PCM}\right) = h_v(\langle T\rangle_{foam} - \langle T\rangle_{PCM}) \tag{4}$$

$$(1-\epsilon)\left(\rho C_p\right)_{foam}\frac{\partial\langle T\rangle_{foam}}{\partial t} + \mathrm{k}_{\mathrm{eff}_{\mathrm{foam}}}\nabla^2\langle T\rangle_{foam} = -h_v(\langle T\rangle_{foam} - \langle T\rangle_{PCM}) \tag{5}$$

Equation (2) is the continuity equation. Equation (3) is the averaged momentum balance equation, where the last two terms on the right side are the Darcy and the Forcheimer terms, respectively. $\bar{\bar{K}}$ is the permeability coefficient, while C_F is Forccheimer coefficient, and they have been determined according to Calmidi [12]. To simulate the phase change in equation (3) and (4), all PCM thermodynamic properties have been defined using a continuous step-function, to improve numerical convergence. In the energy balance equations (4) and (5), $h_v$is the volumetric heat transfer coefficient, and is defined as

$$h_v = h_{sf}a_s \tag{6}$$

where h_{sf} is the Interfacial Heat Transfer Coefficient (IHTC), while a_s is the specific surface area of the metal foam.

2.3. Interfacial heat transfer coefficient (IHTC) determination

The interfacial heat exchange coefficient (h_{sf}) is usually estimated using existing correlation for tubes in cross flow ([13], [14]). These approaches can lead to incorrect results since such correlations have not been obtained for paraffin embedded in metal foam, and do not take into account the different phases in the melting process (i.e. preheating, melting and liquid convective phases).

Another interesting approach was proposed by Mesalhy et al. [6], who assumed the porous matrix geometry to be an intersected mesh of fibres with circular cross section area. The IHTC was then calculated by simplifying the heat exchange between matrix layer and PCM as heat conduction in two cylindrical layers. The correct estimation of this coefficient is important because it deeply affects the phase change process. In order to understand how much the volumetric heat transfer coefficient h_v affects the melting front behaviour, a sensitivity analysis was performed. The results show that there is a threshold value of the volumetric heat transfer coefficient: for higher values, the temperature difference between the metal foam and the PCM is negligible, so a LTE and a LTNE model give basically the same results; for lower values the position of the melting front highly depends on the h_v value. From equation (4) the threshold value depends on:

- the local thermal diffusivity of the PCM;
- the thermal gradients and temperature time derivatives.

In this paper, a new modelling approach for the IHTC calculation is proposed. Three coefficients have to be determined, because three different conditions occur during the phase change process:

- heat exchange between solid PCM and metal foam that occurs when $\langle T \rangle_{foam}$ is lower than $T_{melt-start}$;
- heat exchange between melting PCM and metal foam that ends when $\langle T \rangle_{PCM}$ becomes higher than $T_{melt-end}$;
- heat exchange between liquid PCM and metal foam that begins once the melting process is over.

2.3.1. *Solid-solid and melting IHTCs determination*

The idea in this study is to use the Kelvin 3D model of the foam structure to calculate the IHTC in the conditions listed before. In fact, under the hypothesis of negligible temperature gradient in a single foam cell element, a uniform time dependent temperature is set as boundary condition on the surface of the paraffin cell in contact with the metal foam. On the remaining surface an adiabatic boundary condition is set (symmetry). The heat transfer coefficient per unit of metallic foam surface can be calculated as the time average of:

$$h_{sf} = \frac{1}{t} \int \frac{\dot{Q}_{par-foam}(t)}{S[T_{foam}(t) - \langle T \rangle_{PCM}(t)]} dt \tag{7}$$

where $\dot{Q}_{par-foam}(t)$is the thermal power at the boundary between the paraffin cell and the metal foam, S is the metal foam surface and $\langle T \rangle_{PCM}$(t) is paraffin cell medium temperature and is defined as:

$$\langle T \rangle_{PCM} = \int_{cell} \frac{T_{PCM} dV}{V_{cell}} \tag{8}$$

This approach has a high computational cost above all to determine IHTCs during melting conditions because a highly non-linear 3D problem has to be solved. For this reason, the IHTC has been determined using a simplified 1D spherical model, following the same conceptual approach shown before. The time dependent temperature imposed on the boundary is supposed to be the average temperature on the surface of the paraffin sphere: the portion in direct contact with the foam is assumed to be at T_{foam}, while the portion that is not in contact with the foam is supposed to be at $\langle T \rangle_{PCM}$. It follows that T_{foam} can be calculated as

$$T(R,t) = (1 - a_c)\langle T\rangle_{PCM}(t) + a_c T_{foam}(t) \tag{9}$$

$$T_{foam} = \frac{T(R,t) - (1 - a_c)\langle T\rangle_{PCM}(t)}{a_c} \tag{10}$$

where a_c is fraction of the cell external area in direct contact with the foam and is defined as:

$$a_c = \frac{A_{foam}}{4\pi R_{cell}^2} = \frac{V_{cell} a_s}{4\pi R_{cell}^2} \tag{11}$$

h_{sf} has to be defined per area of metal foam surface, so substituting eq. (10) in eq. (7) it follows

$$h_{sf} = \frac{1}{t_f}\int_0^{t_f}\left(\frac{\dot{q}_{par-foam}(t)\cdot a_c}{T(R,t) - \langle T\rangle_{PCM}(t)}dt\right)\left(\frac{1}{a_c}\right) \tag{12}$$

where $T(R,t)$ is the imposed boundary condition of the 1D model and $\dot{q}_{par-foam}$ is the heat flux normalized on the whole paraffin sphere surface; t_f in case of melting heat exchange is the time when the temperature at the cell center becomes higher than $T_{melt-end}$, (i.e. when melting process is concluded) while in case of solid-solid heat exchange has been assumed arbitrarily to be $100s$.It can be verified that h_{sf} shows little dependence from the function imposed as boundary condition ($T(R,t)$), as can be understood from Table 1.

Table 1.$\boldsymbol{h_{sf}}$calculated for various boundary conditions for a 10 PPI 95% porosity cell.

Solid-solid heat exchange Function $T(R,t)$	$h_{sf}[W/(m^2K)]$	Melting heat exchange Function $T(R,t)$	$h_{sf}[W/(m^2K)]$
$298 + 0.02t + 0.005t^2$	337.71	$300 + 0.01t$	335.84
$298 + 0.1t$	314.95	$300 + 0.01t + 0.0002t^2$	365.47
$298 + 2\log(t+1)$	286.67	$300 + 2\log(t+1) + 0.01t$	290.02

Notice that h_{sf} does not vary significantly between melting and solid–solid conditions. For this reason, this coefficient will be assumed to be constant in both phases.

The 1D approach was numerically validated for the simplest case of solid-solid heat exchange that occurs before melting process starts. The results obtained with the 1D model are compared with those obtained with a 3D transient model of the heat conduction in a single cell. Table 2 reports the IHTCs obtained for the 85% porosity foam at various PPI with both 3D and 1D model.

Table 2.IHTC comparison for various PPI for an 85% porosity metal foam calculated with the 1D and the 3D model.

Porosity ε	PPI	Cell diameter [m]	$h_{sf}[W/(m^2_{foam}K)]$ 3D model	$h_{sf}[W/(m^2_{foam}K)]$ 1D model
85%	10	0,00623	271	257
	20	0,00312	550	495
	30	0,00156	1077	1048

2.3.2. *Convective IHTC determination*

When the paraffin wax is completely melted, natural convection can occur. To determine the heat transfer coefficient in this condition, the magnitude of the velocity field induced has to be estimated. To do so, the volume averaged model was solved with a first try IHTC to determine the order of magnitude of the velocity field. In order to determine the interfacial heat transfer coefficient during the liquid-solid heat exchange, a 3D stationary model was solved (see figure 2).

Table 3. IHTC during natural convection for various velocity inlet conditions.

u_o[m/s]	$\varepsilon = 0.94;\ 10\ PPI$ $h_{sf}[W/(m^2K)]$	$\varepsilon = 0.94;\ 20\ PPI$ $h_{sf}[W/(m^2K)]$	$\varepsilon = 0.94; 0\ PPI$ $h_{sf}[W/(m^2K)]$
$1 \cdot 10^{-5}$	293.4	596.7	1194.3
$5 \cdot 10^{-5}$	281.4	568.6	1138.4
$1 \cdot 10^{-4}$	340.4	690.5	1367.1
$5 \cdot 10^{-4}$	344.6	704.4	1453.8

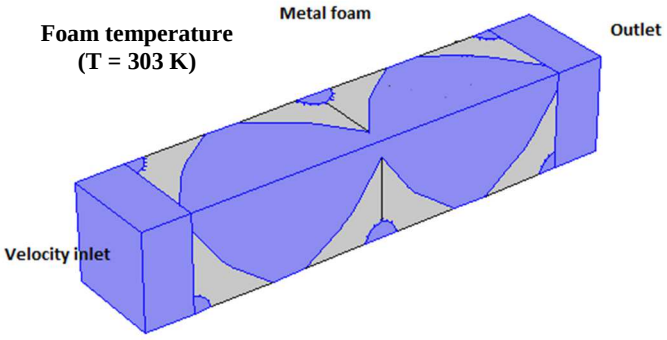

Figure 2. Schematic representation of the 3D stationary for the IHTC calculation during natural convection. The different boundary conditions for both fluid-dynamic and thermal model are reported.

Mass, momentum and energy equations are solved. For the momentum equation, the velocity found with the first iteration is used as inlet boundary condition for the simulation. No slip condition is used at the solid/fluid interface. At the outlet, the atmospheric pressure is assumed. For the energy equation, a uniform ambient temperature is assumed at the fluid inlet, while a uniform temperature value of 303 K is employed at the solid fluid interface. Symmetry condition is used on the other boundary surfaces.

The finite element commercial code COMSOL Multiphysics is employed to solve the governing equations and boundary conditions. In Table 3 are reported the IHTCs calculated for velocity inlet conditions close to the one calculated after the first iteration.

3. Model validation and results

In order to validate the model developed, the experimental data by Lafdi et al. [7] have been considered. The system was heated from the left side and cooled by a heat sink on the right side using an aluminum plate chilled by flowing water. The validation is only qualitative and not quantitative, because of the uncertainty on the boundary conditions on the heater side and on the heat sink side. In fact, it is not possible to estimate the contact resistance between heater plate and metal foam that can play an important role during the dynamic of the melting process, and the thermal power absorbed by the heat sink. Moreover, the experimental characterization of the apparent specific heat during phase change is not reported in the article. Therefore, it was assumed that the specific heat-temperature function during phase change has to be a continuous Dirac Delta function.

Table 4.IHTC during and coupling coefficients during melting and solid-solid heat exchange.

	$\varepsilon = 0.94$				
	h_{sf}		$a_s[m^2/m^3]$	$h_{sf}a_s[W/m^3]$	$h_{sf}a_s[W/m^3]$
PPI	Solid-solid	Melting		Solid-solid	Melting
10	314.7	368.2	511.24	$1.61 \cdot 10^5$	$1.88 \cdot 10^5$
20	626.2	678.5	1022.48	$6.40 \cdot 10^5$	$6.94 \cdot 10^5$
40	1388	1353	2044.97	$2.84 \cdot 10^6$	$2.77 \cdot 10^6$

The chosen comparison parameters are melting front shape after 80 minutes (4800 s) and the heater plate temperature evolution. For a further model validation, we are planning our own experimental campaign, where metal foam and heated plate will be brazed, in order to reduce as much as possible, the contact resistance. Table 4 shows the IHTCs and the coupling coefficient that have to be inserted in equations (3) and (4) for the melting and solid-solid heat exchange.

Table 5. Metal foam effective properties.

Metal foam effective properties $\boldsymbol{\varepsilon = 0.94}$	10 PPI	20 PPI	40 PPI
Effective thermal conductivity $[W/mK]$	3.67		
Density $[kg/m^3]$	162		
Forchheimer coefficient	0.0153		
Foam permeability $[1/m^2]$	$1.037 \cdot 10^{-7}$	$2.583 \cdot 10^{-8}$	$6.458 \cdot 10^{-9}$

Comparing the results shown in table 4 with those in Table 3, it is possible to assume a constant IHTC for all the heat exchange phases for each case, since the values obtained are similar and differ about 10%. This assumption does not affect the calculation precision but reduces the calculation time, because IHTC is now a constant value instead of a temperature depending function. The system is heated with a constant and uniform heat flux (28.9 W). The thermal power was supposed to be completely delivered to the metal foam, since its effective conductivity is much higher than paraffin one (see table 3 in [7]). Foam effective thermal conductivity was calculated according to (12), as suggested by the supplier (ERG Aerospace) [15].

$$k_{eff} = \frac{1-\varepsilon}{3} k_{Al} \tag{13}$$

The heat sink was simulated imposing the initial temperature at the corresponding boundary for all the modelled cases. The experimental data shows that the mean temperature on the heater plate is generally lower for lower PPI foams. This trend is in good agreement with the experimental data, as can be seen comparing figures 3a and 3b.

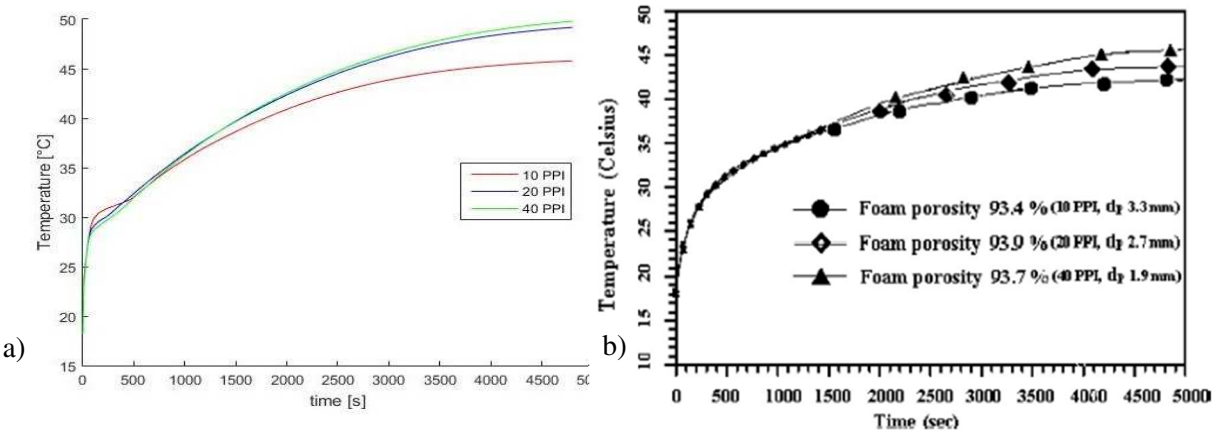

Figure 3. Comparison between experimental and mathematical results of heater temperature.

Moreover, with the 10 PPI foam a steady state condition is achieved before the other two cases in both experimental and model results. In fact, even if the coupling coefficient is lower for lower PPI foams, the permeability factor increases as well as the heat transferred because of natural convection.

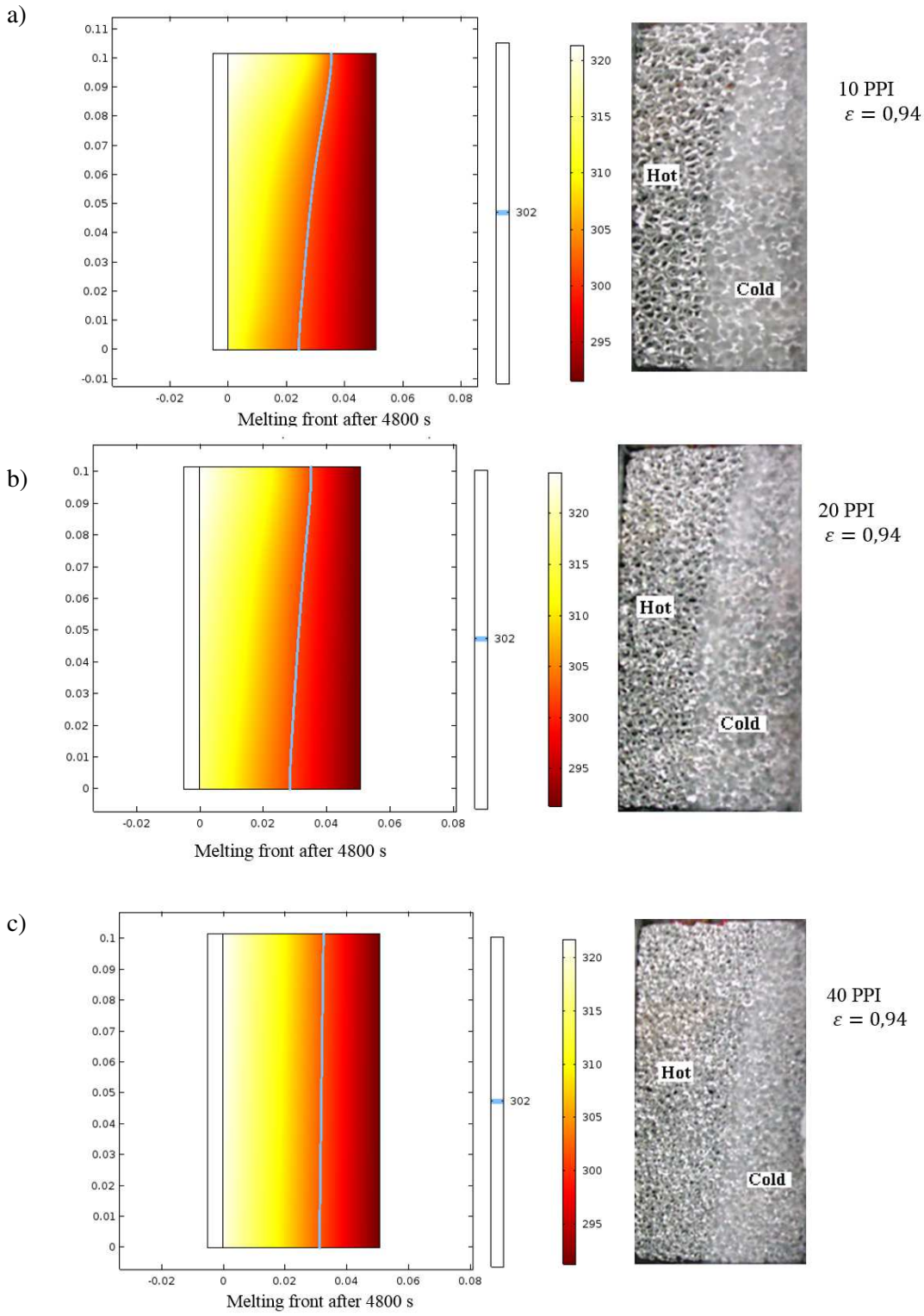

Figure 4.Comparison between experimental and model melting front after 4800 s. The grey line identifies the melting front in the model results.

Analysing the 10 PPI foam temperature contour, there are areas where paraffin is hotter that metal foam. The importance of convective heat transfer can be also seen from the melting front shape that is much more irregular for the 10 PPI foam. Figure 4 shows a comparison between the model and the experimental melting front for the 10 PPI, 20 PPI and 40 PPI foams. The higher IHTC typical of higher

PPI foams seems to have little influence on heater temperature in the cases analysed. This happens because of the low thermal flux that has to be dissipated. Notice that in order to have a further validation on the IHTCs calculated, a higher thermal power should be furnished to the system.

4. Conclusions

A numerical model based on solving the volume averaged conservation equations for mass, momentum and energy with phase change (melting) is developed in order to study the effect of adding a high thermal conductivity matrix on the performance of PCM energy storage. The convection motion of the liquid phase inside the porous matrix is solved considering the Darcy, Brinkman and Forcheimer effects. The local thermal non-equilibrium assumption is considered due to the large differences in thermal properties between the solid matrix and PCM by applying a two-energy equation model. A novel model to calculate the interfacial heat transfer coefficient (IHTC) is proposed by simulating heat exchange between the PCM and the Kelvin ideal metal foam. For the solid-solid and the melting heat exchange phase the 3D transient model was simplified with a 1D transient model to reduce computational cost. This approach was numerically validated since the results obtained with the 1D model are very close to the 3D model ones in the case of solid-solid heat exchange. For the liquid phase a 3D stationary model was solved for different velocity inlet conditions. The interfacial heat transfer condition is similar for the three cases analysed, so a constant value has been chosen for the simulation. The results of the averaged equations showed good agreement with the experimental results found in literature as for the melting front shape and heater temperature evolution, but an experimental setup will be built in order to further validate the model developed. With the coupling coefficient calculated, a microgravity condition model was built and the results were compared with the ones previously obtained.

Nomenclature

a_s	Specific foam area per unit of volume $(1/\mathrm{m})$
a_c	Paraffin cell area fraction in contact with foam $(\mathrm{m}^2_{\mathrm{foam}}/\mathrm{m}^2_{\mathrm{cell}})$
C_F	Forcheimer coefficient
C_p	Specific Heat (W/kg·K)
d_c	Cell diameter (m)
$\mathrm{d_p}$	Pore diameter (m)
g	Gravity acceleration (m/s^2)
h_{sf}	Interfacial heat transfer coefficient (W/m^2·K)
h_v	Volumetric heat transfer coefficient (W/m^3·K)
k	Thermal conductivity (W/m·K)
$\overline{\overline{\mathrm{K}}}$	Porous medium permeability (1/m^2)
L	Latent heat of fusion (J/kg)
m	Mass (kg)
p	Pressure (Pa)
$\dot{q}_{par-foam}$	Heat flux on the paraffin cell boundary (W/m^2)
$Q_{par-foam}$	Thermal power exchanged between paraffin and metal foam (W)
S	Surface (m^2)
T_{PCM}	PCM temperature (K)
$T_{start-melt}$	Initial melting temperature (K)
$T_{end-melt}$	Final melting temperature (K)
T_{foam}	Foam temperature (K)
T(R,t)	Temperature imposed for $\mathrm{h_{sf}}$ determination (K)
t	Time (s)
t_f	Time of simulation for $\mathrm{h_{sf}}$ determination (s)
$\bar{v}$	Velocity vector (m/s)
V	Volume (m^3)
V_{cell}	Metal foam cell volume (m^3)

Abbreviations

IHTC	Interfacial Heat Transfer Coefficient
PPI	Pore Per Inch
LTNE	Local Non Thermal Equilibrium
LTE	Local thermal equilibrium
VAT	Volume Averaging Technique
REV	Representative Volume Element
IR	Impregnation Ratio
PCM	Phase Change Material
TES	Thermal Energy Storage

Greek symbols

ε	Porosity
μ	Dynamic viscosity (kg/m^2·s)
ρ	Density (kg/m^3)
β	Volume expansion coefficient (1/K)

Other symbols

x, *y*, *z*	Coordinates (m)
<>	Volume average

References

[1] Fan L and Khodadadi J M 2011 Thermal conductivity enhancement of phase change materials for thermal energy storage: A review *Renewable and Sustainable Energy Reviews* **15 (1)** 24-46.

[2] Tian Y and Zhao CY 2011 A numerical investigation of heat transfer in phase change materials (PCMs) embedded in porous metals *Energy* **36 (9)** 5539–5546.

[3] Tong X Khan J A and Amin M R 1995 Enhancement of solidification heat transfer by inserting metal-matrix into phase change material Proceedings of the 1995 *ASME International Mechanical Engineering Congress & Exposition San Francisco, CA, USA 1 1-8.*

[4] Mancin S Diani A Doretti L Hooman K and Rossetto L 2014 Experimental analysis of phase change phenomenon of paraffin waxes embedded in copper foams *International Journal of Thermal Sciences* **90** 79-89.

[5] Alshaer W G Nada SA Rady M A Le Bot C and Del Barrio EP2014 Numerical investigations of using carbon foam/PCM/Nano carbon tubes composites in thermal management of electronic equipment *Energy Conversion and Management* **89** 873–884.

[6] Mesalhy O Lafdi K Elgafy A and Bowman K (2005), Numerical study for enhancing the thermal conductivity of phase change material (PCM) storage using high thermal conductivity porous matrix *Energy Conversion and Management* **46(6)** 847-867.

[7] Lafdi K Mesalhy O and Shaikh S 2007 Experimental study on the influence of foam porosity and pore size on the melting of phase change materials *Journal of Applied Physics* **102 (8)** paper number 083549.

[8] Weaire D and Phelan R 1994 A counter-example to Kelvin's conjecture on minimal surfaces *Philosophical Magazine Letters* 69107–110.

[9] Cunsolo S Iasiello M Oliviero M Bianco N Chiu W K and Naso V 2016 Lord Kelvin and Weaire–Phelan Foam Models: Heat Transfer and Pressure Drop *Journal of Heat Transfer* **138 (2)** paper number 022601.

[10] Iasiello M Cunsolo S Oliviero M Harris W M Bianco N Chiu W K and Naso V 2014 Numerical Analysis of Heat Transfer and Pressure Drop in Metal Foams for Different Morphological Models *Journal of Heat Transfer* **136 (11)** paper number 112601.

[11] Whitaker S 1999 The method of volume averaging (Norwell, MA, USA: Kluwer Academic Publishers).

[12] Calmidi V 1998 Transport phenomena in high porosity metal foams Ph.D thesis: University of Colorado.

[13] Liu Z Yao Y and Wu H 2013 Numerical modelling for solid–liquid phase change phenomena in porous media: Shell-and-tube type latent heat thermal energy storage *Applied Energy* **112** 1222–1232.

[14] Li W Q Qu Z G He Y L and Tao W Q 2012 Experimental and numerical studies on melting phase change heat transfer in open-cell metallic foams filled with paraffin *Applied Thermal Engineering* **37** 1-9.

[15] http://www.ergaerospace.com/Thermal-transfer.html.